Biosensors and Bioelectronics 72 (2015) 268–274

Contents lists available at ScienceDirect

Biosensors and Bioelectronics

journal homepage: www.elsevier.com/locate/bios

Gold nanoparticle incorporated inverse opal photonic crystal capillaries for optofluidic surface enhanced Raman spectroscopy

Xiangwei Zhao [a,b,*], Jiangyang Xue [a,b], Zhongde Mu [a,b], Yin Huang [c], Meng Lu [c,**], Zhongze Gu [a,b,*]

[a] State Key Laboratory of Bioelectronics, School of Biological Science and Medical Engineering, Southeast University, Nanjing 210096, China
[b] Laboratory of Environment and Biosafety Research Institute of Southeast University in Suzhou, Suzhou 215123, China
[c] Department of Electrical and Computer Engineering, Iowa State University, Ames, IA 50011, USA

ARTICLE INFO

Article history:
Received 18 March 2015
Received in revised form
12 May 2015
Accepted 13 May 2015
Available online 14 May 2015

Keywords:
Inverse opal photonic crystal (IO PhC)
Optofluidics
Surface enhanced Raman spectroscopy (SERS)
Point-of-care testing (POCT)

ABSTRACT

Novel transducers are needed for point of care testing (POCT) devices which aim at facile, sensitive and quick acquisition of health related information. Recent advances in optofluidics offer tremendous opportunities for biological/chemical analysis using extremely small sample volumes. This paper demonstrates nanostructured capillary tubes for surface enhanced Raman spectroscopy (SERS) analysis in a flow-through fashion. The capillary tube integrates the SERS sensor and the nanofluidic structure to synergistically offer sample delivery and analysis functions. Inside the capillary tube, inverse opal photonic crystal (IO PhC) was fabricated using the co-assembly approach to form nanoscale liquid pathways. In the nano-voids of the IO PhC, gold nanoparticles were in situ synthesized and functioned as the SERS hotspots. The advantages of the flow-through SERS sensor are multifold. The capillary effect facilities the sample delivery process, the nanofluidic channels boosts the interaction of analyte and gold nanoparticles, and the PhC structure strengthens the optical field near the SERS hotspots and results in enhanced SERS signals from analytes. As an exemplary demonstration, the sensor was used to measure creatinein spiked in artificial urine samples with detection limit of 0.9 mg/dL.

1. Introduction

Point-of-care testing (POCT) is featured by its ability to perform "near the patient" and real-time detections without the involvement of laboratory staff and facilities (Gervais et al., 2011; Gubala et al., 2012). The POCT devices are expected to be capable of analyzing complex human body fluids such as blood, urine, saliva that contain disease related molecules, metabolites, drugs, and electrolytes. There are a few hurdles to overcome towards the implementation of POCT devices for the practical problems. For example, it is desirable to perform the measuring using minimal amount of sample and reagent; it is also important to simplify the sample preparation and minimize human interferences; and the detection of multiple analytes is a key feature for the diagnostics of complex diseases, like cancers and cardiovascular diseases. The rapid development of microfluidics and nanotechnology makes it possible to perform biological/chemical analysis on a chip scale and provides unprecedented opportunities to bridge the gaps between the "in lab" technology and the "on site" applications. Meanwhile, the efforts to miniaturize photonic systems allow the implementation of optical spectroscopic approaches in POCT systems. With optical components, such as emitter, detector, sensors, seamlessly integrated with fluidic system, sample process and optical detection become more compact and efficient (Schumacher et al., 2012; Surdo et al., 2012; Wade and Bailey, 2014; Zhu et al., 2013). The combination of optics and microfluidics leads to the emerging of the optofluidics, which provide synergistic benefits on the performance and functions between microfluidics and photonics (Fan and White, 2011; Schmidt and Hawkins, 2011).

Optical-spectroscopy approaches are capable of distinguishing molecules by their structural fingerprints. In addition, the amplification of optical signal are gained owing to the nanostructures of photonic components, which can greatly enhance interaction probabilities of analytes and sensor as well as the interaction of light and matter in the transducing procedure (Chanda et al., 2011; Ganesh et al., 2007; Hou et al., 2014; Shen et al., 2012). For example, recently surface enhanced Raman scattering/spectroscopy (SERS), which can provide molecular fingerprint information of analytes, is more and more widely adapted (Schlucker 2014). This

* Corresponding authors at: State Key Laboratory of Bioelectronics, School of Biological Science and Medical Engineering, Southeast University, Nanjing 210096, China.
** Corresponding author.
E-mail addresses: xwzhao@seu.edu.cn (X. Zhao), menglu@iastate.edu (M. Lu), gu@seu.edu.cn (Z. Gu).

http://dx.doi.org/10.1016/j.bios.2015.05.036
0956-5663/

is especially true in optofluidics when delicate plasmonic structures which can support enhanced electromagnetic fields needed for SERS are designed and fabricated by processes compatible with those of microfluidics chips (Alba et al., 2013; Oh and Jeong, 2014; Sun et al., 2014; Wang et al., 2014). However, the enhanced intensity of electromagnetic fields of plasmonic structures cannot guarantee the efficiency of SERS if the analytes didn't reach the enhanced vicinity of the structure and interact with them efficiently.

Therefore, kinds of measures were adopted to enhance the effective SERS signal by increasing the probability of analyte encountering with the near-field of the plasmonic sensitive surface or "hot spots". For example, De Angelis et al. detected the SERS signal of few molecules by localizing the analyte-containing droplet onto a plasmonic probe on an artificial super-hydrophobic surface and concentrating the analytes on the tip of the probe via evaporation (De Angelis et al. 2011). In microfluidic chip applications, Khaing Oo et al. used Au-NP immobilized multihole capillaries, which can provide 3-D flow-through structures to accommodate much more available SERS-active sites interaction with analytes, for rapid and sensitive SERS detection (Guo et al., 2012; Oo et al., 2012). Yazdi et al. trapped silver nanoparticle and analyte conjugates by 15 μm packed silica microspheres in a microfluidic channel to get the SERS signal of flow-through analytes and improved the detection limit by more than four orders of magnitude as compared with an open microfluidic channel (Yazdi and White, 2012). However, their microfluidic channel sizes are still in the micron scales in which laminar flow retards the diffusion of analytes and limits their interaction with plasmonic structures in nanoscale. In addition, the need for formation nanoparticle–analyte conjugates by electrostatic interaction constrains the scope of SERS applications.

Inverse opal photonic crystal (IO PhC) has periodic structure in three dimensions, which can be used for the modulation of light propagation since its period is equivalent to the light wavelength (Schroden et al., 2002). The nano-voids of IO PhC are interconnected to form tortuous nanofluidic channels with a high surface to volume ratio, which offers nano-confinement environments for analyte and nanoparticle interactions. All these characters make IO PhC a good candidate material for optofluidic chips especially in POCT. Hence, in this paper, we proposed a simple and cost-effective method to make IO PhC in micro-capillaries and incorporate gold nanoparticles in the nano-voids of IO by in situ synthesis for optofluidic SERS analysis. As illustrated in Scheme 1, first, binary particle solution of silica and polystyrene (PS) were infiltrated into a capillary by capillary force and dried to form an opaline photonic crystal with silica colloids fill up the interstices of the PS nanoparticles. And then the PS nanoparticles as template were removed by calcination to get IO PhC, in the nano-voids of which gold nanoparticles were synthesized in situ. Finally, analyte solution was perfused into the capillary for SERS analysis.

2. Materials and methods

2.1. Materials and reagents

Monodispersed polystyrene nanoparticles are purchased from Nanjing Dongjian Biotechnolgoy Co., Ltd. (China). 7 nm SiO_2 nanoparticles (LUDOX SM) and (3-aminopropyl)triethoxysilane (APTES) are purchased from Sigma Aldrich (US). Capillaries are purchased from Polymicron Technology™ (US). Hydrochloroauric acid ($HAuCl_4$) and 4-Aminothiophenol (4-ATP) are purchased from Sinopharm Chemical Reagent Co., Ltd. (China). Sodium citrate is purchased from Shanghai Chemical Reagent Co., Ltd. (China). Artificial urine and Creatinine are purchased from Huzhou InnoReagents Co., Ltd. (China).

2.2. Preparation of inverse opal photonic crystal in capillaries

5 cm quartz capillaries with inner diameter of 180 μm were first calcinated at 500 °C to remove the polyimide coating and washed with acetone and ethanol respectively. Then they were treated with piranha solution (a 3:1 mixture of concentrated sulfuric acid with hydrogen peroxide, which is dangerous and should be handled with care) and dried with nitrogen after washing.

Inverse opal photonic crystals were prepared by co-assembly of monodispersed polystyrene (PS) and silica (SiO_2) nanoparticles in the capillaries. In our experiment, four sizes of 5% PS nanoparticles (185 nm, 236 nm, 269 nm and 307 nm) in aqueous suspension and 7 nm SiO_2 nanoparticles (LUDOX SM, Sigma Aldrich) whose concentration was adjusted to 5% were used. After the monodispersed PS and SiO_2 nanoparticles were mixed thoroughly, they were infiltrated into the capillaries by capillary force and dried at room temperature. The mixing ratio of PS and silica nanoparticles was optimized between 2:1 and 7:1 so that ordered self-assembled structures were obtained in capillaries. Then the capillaries were sintered at 550 °C for 3 h with a heating/cooling ramp of 1 °C/min to remove the PS nanoparticles and inverse opal photonic crystals were generated. The PhC nanostructures were observed with a field emission scanning electron microscope (FESEM, Zeiss Ultra Plus, Germany).

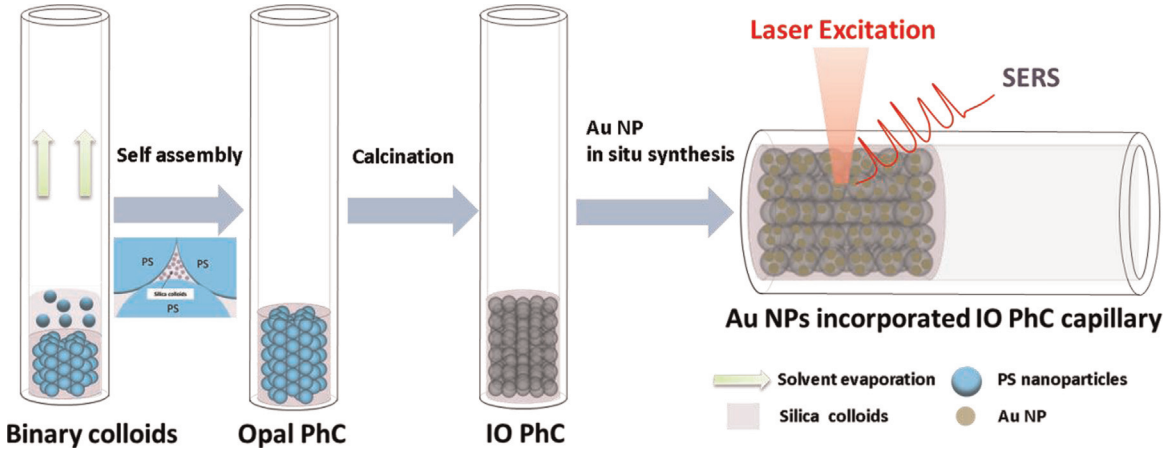

Scheme 1. Schematic fabrication of gold nanoparticle incorporated inverse opal photonic crystal (IO PHC) capillary for SERS.

2.3. In situ synthesis of gold nanoparticles in IO PhC capillary

First, the IO PhC capillaries were treated with Piranha solution for 12 hours and 5% APTES in ethanol solution for 6 hours subsequently to graft amino groups on the surfaces of the nano-voids in the IO PhC. Then 1000:4 (V/V) mixture solution of 0.01% $HAuCl_4$ and 1% Sodium Citrate were injected at a velocity of 10 μL/min into the IO PhC at 80 °C for 60 min to synthesize gold nanoparticles in the nano-voids of IO PHC. At last, the IO PhC capillaries were washed with pure water before SERS applications.

2.4. Raman measurement

The Raman signals were collected with a desktop Raman Spectrometer (PeakSeeker Pro 785E, Oceanoptics, USA) coupled to a microscope with a 50× objective through an optical fiber. The NIR diode laser (λ_{exc}=785 nm and output power of 5 mW) was focused on the detection area from the side of the capillary tube. The exposure times were set as 3 s. For each measurement, the samples were measured 3 times and the acquired Raman spectra were averaged to reduce the random noise.

2.5. Numerical simulation

A commercial software package (FDTD Solutions, Lumerical Solutions Inc.) was used to simulate the optical responses of the IO PhC structures with AuNPs. The simulated structure consisted of a face center cubic IO photonic crystal with the lattice constant of 280 nm. Two AuNPs with diameter of 80 nm were placed inside each opal and the gap between them is 40 nm. In the *x*–*y* plane, periodic boundary conditions were imposed to truncate the periodic structure at *x* and *y* boundaries. Perfectly matched layers are imposed at boundaries of the propagation direction (*z* direction) to properly absorb outgoing radiation. The simulation included 15 layers of nano-voids along the *z* direction. The structure was excited by a normally incident, unit magnitude plane wave propagating in the *z* direction. The near field distributions at a given wavelength were plotted along the center cross-sectional plane of the IO PhC structure.

3. Results and discussion

3.1. Inverse opal photonic crystal fabrication in capillaries

During the co-assembly of binary particle of PS and silica, the small silica colloids will fill the interstices of the large PS nanoparticles as template. Therefore, in order to obtain ordered PhC structure, the volume ratio of the PS and silica should be optimized. In our experiment, six volume ratios are tried from 2:1 to 7:1 to form columns of co-assembly in capillaries. Fig. 1(a)–(d) are the end face structure of the co-assembly of 269 nm nanoparticles and 7 nm silica colloids at four different volume ratios after remove of the PS nanoparticles by calcination at 550 °C. It can be seen that between 5:1 and 7:1, the co-assemblies are more ordered and the nano-voids derived from the PS nanoparticles are arranged in hexagonal packing. And in Fig. 1(c), when the ratio is 6:1, a typical IO PhC of FCC (face centered cubic) lattice is formed with a reflection peak at 568 nm. However, at the other end of the other end of the IO PhC column the measured reflection peak is 556 nm which means that the ratio is not the best. Hence, by further fine tune of the volume ratio at 5.5:1, uniform IO PhC columns are obtained in capillaries with reflection peaks of both ends at 559 nm. Fig. 1(e) is one cross section of the IO PhC in the capillary which confirms the FCC structure. In Fig. 1(f) are four IO PhC capillaries with inner diameter of 180 μm made from 185 nm, 236 nm, 269 nm and 307 nm PS templates. For visualization the capillaries are infiltrated with water to display the reflection color of the IO PhC except for the IO PhC from 185 nm PS template whose reflection peak is not in the range of visible. It can also be judged that by the as proposed binary particle co-assembly method, uniform IO PhC structure can be obtained reliably. While in POCT applications, microfluidic technologies are more and more favorable because of the limited sample amount and the analytical advantages owing to reduced sizes. In this regard, capillaries as preformed microchannels with various sizes are of good choice not only because of the low cost but also because of the convenient connection with microfluidic chips and tubings. In our method, the capillaries are filled with porous IO PhC composed of nano-voids of hundreds nanometers with interconnecting pores. As can see from Fig. 1(c) and (e), the size of interconnecting pores is about 1/3 of that of the nano-voids. And both of them form zigzag nanofluidic channels in the capillary, which provides high surface to volume ratio and enhances the possibilities of analyte and gold nanoparticle interactions incorporated in the confined nanochannels.

3.2. In situ synthesis of gold nanopartles in IO PhC capillary

In order to make the full use of the nanochannels in IO PhC capillary for SERS, an in situ synthesis strategy by reduction of chloroauric acid ($HAuCl_4$) is employed to decorate nano-voids of IO PhC with gold nanoparticles. Since the volume of single nano-void is about 2×10^{-5} pL for IO made from 236 nm PS template, it is

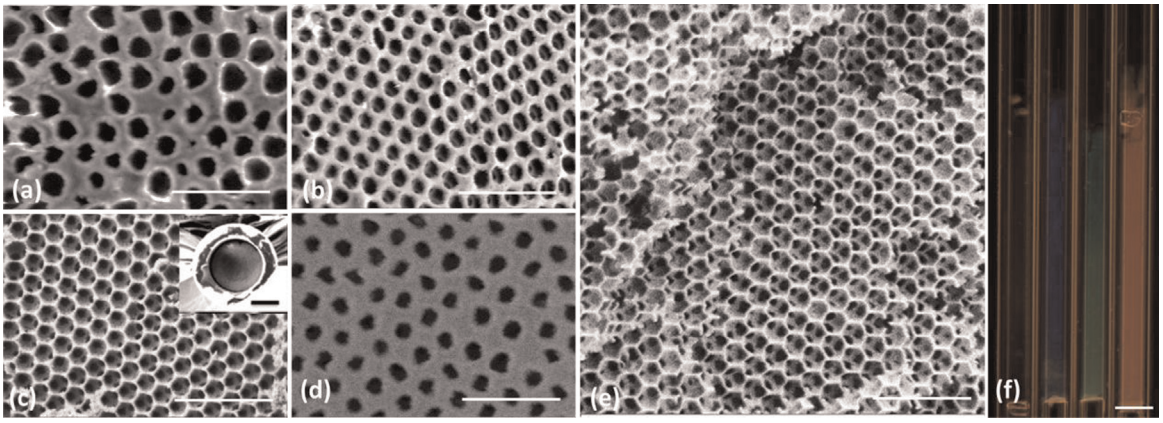

Fig. 1. Nano- and micro-structures of IO PhC capillaries. (a)–(d) SEM images of the end face structure of co-assembly of 269 nm nanoparticles and 7 nm silica colloids mixed at volume ratio of 4:1, 5:1, 6:1 and 7:1 in capillaries, inset of (c) is the capillary end face; (e) the cross section of the structure inside the capillary of (c); (f) picture of four IO PhC capillaries; Scale bar in (a)–(e) is 1 μm, the scale bar in inset of (c) and (f) is 200 μm.

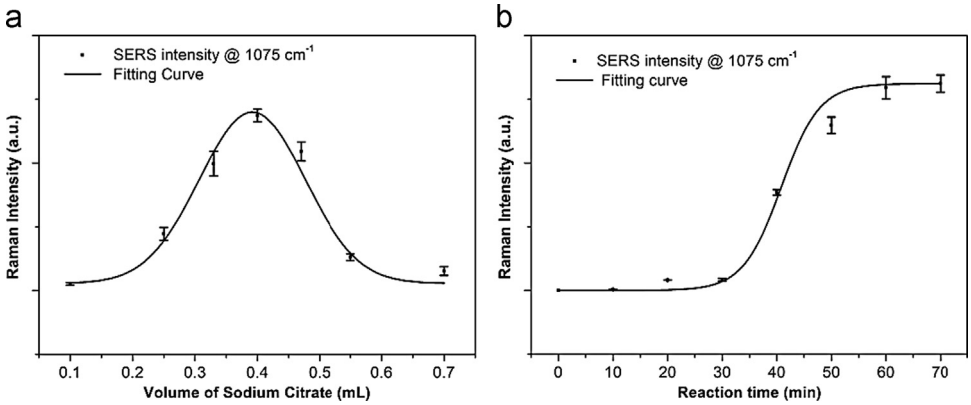

Fig. 2. Effect of different in situ synthesis conditions on the SERS signal of 4-ATP. Raman scattering intensity at 1075 cm^{-1} with different volume of sodium citrate (a) and different reaction time (b).

obvious that the gold source should be continuously supplemented to obtain gold nanoparticles big enough for SERS. Therefore, in our experiment, mixture of 0.01% $HAuCl_4$ and 1% mild reducer sodium citrate are injected at 10 μL/min for certain time through the IO PhC capillary at 80 °C to generate gold nanoparticles in the nano-voids. And the nano-void surfaces are modified with amino groups for the anchoring of gold seeds by electrostatic force during nanoparticle growth. We use 10^{-6} mol/L 4-ATP (4-aminothiophenol) as a Raman probe with characteristic Raman peak at 1075 cm^{-1} to evaluate the SERS performance of the IO PhC capillary incorporated with gold nanoparticle synthesized with different reducer amount and reaction time. As shown in Fig. 2, for IO PhC capillaries from 236 nm PS nanoparticle templates, the volume of $HAuCl_4$ solution is fixed at 100 mL. When the volume of sodium citrate solution varies from 0.1 mL to 0.7 mL, the Raman intensity of 4-ATP fits a parabolic curve and the best volume ratio of $HAuCl_4$ to sodium citrate is 100:0.40 (Fig. 2(a)). At the same time, it is found that the Raman intensity increases quickly after reaction for 30 min but no longer increases after 60 min and it fits a typical S type reaction curve (Fig. 2(b)). Therefore, all the reaction time of in situ synthesis of gold nanoparticles for the following applications is fixed at 60 min. The size and distribution of the gold nanoparticles in the IO PhC are checked by SEM (Fig. S1). When the volume ratio of $HAuCl_4$ to sodium citrate is 100:0.70, 100:0.55, 100:0.40 and 100:0.25, the size of the gold nanoparticles is 20–30 nm, 40–50 nm, 60–80 nm and 100–120 nm respectively. And there are averagely two nanoparticles per nano-void when the volume ratio is 100:0.40. Since the size of interconnecting pores between adjacent nano-voids of 236 nm is about 70 nm, which is relevant to the size of the nanoparticles, there are great possibilities that the two nanoparticles forms dimers by the flow of the analyte solution during analysis. It is reported that the 60 nm gold nanoparticles have better SERS effect and gaps between nanoparticles will provide higher enhance factor than single nanoparticle (Krug et al. 1999). That maybe explains why the SERS performance of IO PhC capillary is better when gold nanoparticles were in situ synthesized at volume ratio of 100:0.40. The SERS performance of three other IO PhC capillaries with nano-void size of 185 nm, 269 nm and 307 nm are also tested and compared after gold nanoparticle incorporation under different volume ratio of reaction solutions. However, the highest Raman intensity at 1075 cm^{-1} comes from the capillaries with 236 nm nano-voids and ~80 nm gold nanoparticles (Fig. S2). Therefore, all the following SERS measurements are carried out on these capillaries.

3.3. Optofluidic SERS detection with IO PhC capillaries

Usually, SERS measurement is performed after the analyte solution is dried on the plasmonic substrate. Since the dried analyte does not distribute uniformly on the substrate and in most cases is not in the vicinity of the hot spots contributing to Raman scattering enhancement, the repeatability and sensitivity of SERS measurement is very poor. What's more, the dry procedure is time consuming and amenable to contaminations. Hence, in case of POCT, direct measurement of the solution sample in nanofluidic channels, which can enhance the possibility of analyte and hot spot interactions, will guarantee the efficiency of SERS analysis especially when the sample is limited and the analyte concentration is low. In order to investigate the kinetics of the SERS analysis, 10^{-6} mol/L 4-ATP, as a usually used SERS probe which can absorb onto Au NPs by thiol group, is injected into the capillaries at velocity of 3 μL/min and the Raman intensity at 1075 cm^{-1} is measured over time. It is found that the Raman intensity increases with time and reaches a plateau after 45 μL (Fig. 3(a)). And the isotherm is like Langmuir isotherm, which indicates a single molecular layer adsorption. Therefore, for analytes that have good affinity to gold nanoparticles, the equilibrium of absorption should be reached for maximum signal. Fig. 3(b) shows the SERS spectra of 4-ATP in ethanol at different concentration from 10^{-9} mol/L to 10^{-5} mol/L after injection with velocity of 3 μL/min and to volume of 50 μL. It can be seen that even at 10^{-9} mol/L the characteristic 4-ATP vibration peaks of C–C stretching, C–H bending and C–C distortion at 1500–1600 cm^{-1}, 1000–1100 cm^{-1} and 300–400 cm^{-1} are detected clearly. It is possible that incubation for a longer time will further enhance the detection limit owing to the analyte absorption on the substrate.

To demonstrate their application in POCT, SERS of creatinine, which is one of the major components of urine and can be used to represent the metabolic and renal function of the human body, is measured using gold incorporated IO PhC capillaries. For analytes that have poor affinity to gold nanoparticles like creatinine, the effect of the flow time and volume on the SERS signal is not obvious. Hence, SERS measurement is performed just after dipping the capillary into creatinine solution and infiltrating the solution by capillary force. Fig. 3(c) shows the SERS spectra of creatinine at different concentrations from 10 mg/dL to 200 mg/dL. Characteristic peaks of creatinine at 628 cm^{-1} (C–H swing), 721 cm^{-1} (H–C=N–H bending), 878 cm^{-1} (N–H bending), 946 cm^{-1} (C–C bending) and 1424 cm^{-1} (C–H stretching/bending) can be detected at 10 mg/dL, which is enough for POCT applications. The average SERS intensities of the characteristic peak at 1424 cm^{-1} were plotted against the concentrations of creatinine using Langmuir fitting (Fig. 3(d)). The limit of detection was calculated to be 0.9 mg/dL (the concentration at which the Raman intensity is equal to the average background signals at 1424 cm^{-1} plus three times the standard deviation), which is much lower than the

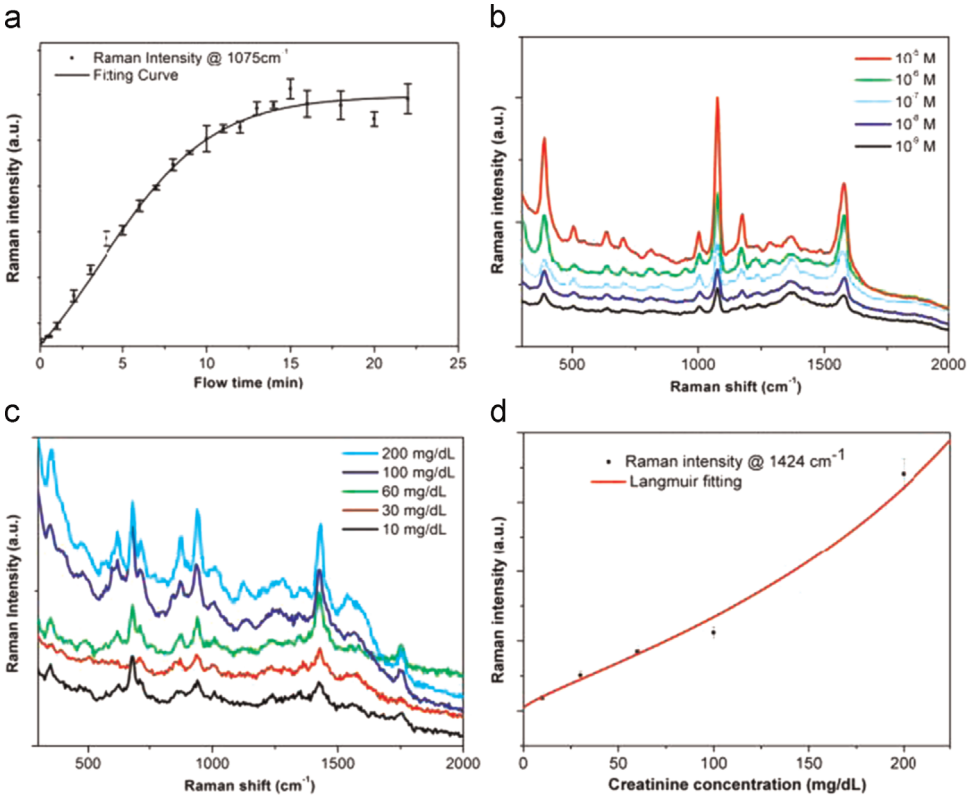

Fig. 3. SERS detection of 4-ATP and creatinine. (a) the intensity variations of Raman peak at 1075 cm^{-1} over time when 4-ATP solution is injected into the capillaries at velocity of 3 μL/min; (b) and (c) SERS spectra of 4-ATP and creatinine at different concentrations; (d) calibration curve of the average SERS intensity measured at 1424 cm^{-1} as a function of creatinine concentration (R^2=0.95468), error bar is calculated with 5 repeats (n=5).

normal concentration of 40 mg/dL. It can be seen that the intensity of Raman signal is proportional to the concentration and the detection range up to 200 mg/dL is adequate for clinical situation according to reference Wang et al. (2010).

Simplicity and rapidness are two features that POCT pursues in order to provide health informations for the prompt judgments of further treatment. And Raman measurement has many advantages over traditional biochemical measurements such as less sample preparations, label-free, reaction independence and quick readout, which has great potential applications in POCT. In our methods, no sample drying procedure is needed and the sample solution can be self-driven into the nanofluidic channels by capillary force followed by directed Raman measurement. What's more, the nanofluidic channel can act as a filter for debris and cells of microns in body fluid samples that could affect the Raman signal. Therefore, the as-proposed gold incorporated IO PhC capillary offers a convenient, sensitive and novel option for POCT in a "dip and measure" fashion.

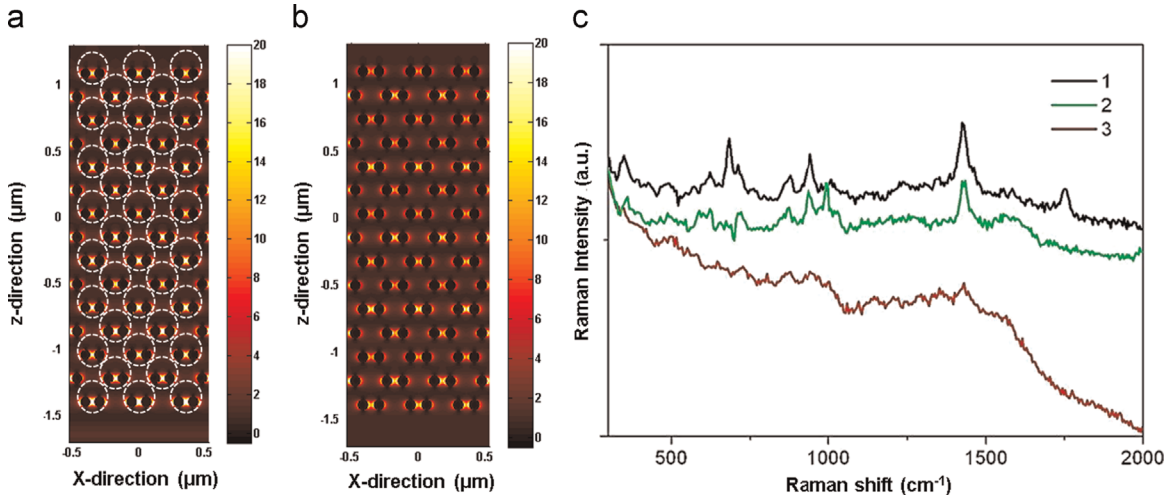

Fig. 4. Numerical simulation and experimental SERS comparison of capillaries with different structures. (a) and (b) is the simulated $|E/E_{inc}|$ profile of gold nanoparticle incorporated IO PhC capillary and gold in capillary excited with 785 nm laser respectively, the white dashed circle outlines the nano-voids of IO PhC; (c) SERS spectra of 60 mg/dL creatinine in artificial urine measured with different substrates; 1, IO PhC capillary incorporated with gold nanoparticle; 2, IO PhC capillary infiltrated with gold nanoparticle and creatinine mixture solution; 3, capillary with gold nanoparticle coated on the inner surface.

3.4. The advantages of IO PhC for Optofluidic SERS

In order to illustrate the advantages of gold incorporated IO PhC capillaries, we simulated the near field distribution of the gold nanoparticles in water within PhC structure and without PhC structure by FDTD as in Fig. 4(a) and (b). It can be seen that the intensity of electric field around gold nanoparticles in PhC structure are higher than that in homogeneous water. The reason may be that the PhC can modulate the electric field distribution by interference of the periodic structure and hence the interaction of light and gold nanoparticles will be enhanced (Fig. S3). The high scattering character of PhC may also account for the enhanced SERS signal. It was reported that excitation wave length at 633 nm is better for SERS measurement based on 60-80 nm gold nanoparticles (Wustholz et al. 2010). However, in our case, the better SERS signal is obtained by 785 nm excitation since the excitation depth is much larger than that of 633 nm as indicated by the simulation (Fig. S4). Hence, 785 nm is chosen as the excitation wavelength although the Raman intensity is proportional to the 4^{th} power of the excitation frequency ($1/\lambda$) (Eric Le Ru, 2008; Schlucker, 2014). In addition the longer excitation wavelength can reduce the effect of fluorescence background, which will be beneficial for Raman spectral signal acquisition.

SERS of 60 mg/dL creatinine measured with three means (Fig. 4(c)) is also compared. The first one uses the as-proposed IO PhC capillary incorporated with Au NPs. The second one uses as-proposed IO PhC capillary infiltrated with creatinine and Au NP mixture solution. The third one uses capillary with Au NPs coated on the inner wall. It is shown that the highest Raman intensities come from the first one and the SERS signal from the third one is so weak that it could hardly be identified. The reason is that the density of "hot spots" on the 2D inner wall of the capillary is much lower than that in the 3D IO PhC. Most of the creatinine molecules are microns away from and beyond the reach of the 2D Au NP layer of the microchannel although the concentration of creatinine is relatively high. In contrast, the distance of the creatinine molecules confined in the nano-voids of IO PhC to the gold nanoparticles and hot spots are in submicron scale, which increases the possibilities of interactions. For the second one, although some characteristic Raman peaks could be detected, uniform occupations of the nano-voids with nanoparticles could not be realized easily. In most cases the IO PhC is jammed with gold nanoparticles. Hence, both the excitation light and scattered Raman signal will be attenuated due to the high intrinsic losses of the metal in spite of the high density of "hot spot". Therefore, in situ synthesis of Au NPs in nano-voids provides a reliably and reproducible way for nanofluidic POCT with both high sensitivity and simplicity of measurements.

4. Conclusions

SERS detection is well known for its ability of revealing the fingerprint of molecules directly in a multiplex and label-free way. Therefore, the combination of micro/nanofluidics and SERS, offers tremendous opportunities for "Sample In, Answer Out" detection with minimum sample processing, which is desirable in POCT applications. In summary, this paper demonstrates nanostructured capillary tubes for SERS analysis in a flow-through fashion. The capillary tube integrates the SERS sensor and the nanofluidic structure to synergistically offer sample delivery and analysis functions. Inside the capillary tube, inverse opal photonic crystal (IO PhC) was fabricated using the co-assembly approach to form nanoscale liquid pathways. On the surface of the IO PhC, gold nanoparticles were in situ synthesized and functioned as the SERS hotspots. The advantages of the flow-through SERS sensor are multifold. The capillary effect facilities the sample delivery process while the nanofluidic channels inside capillary boost the interaction of analyte and gold nanoparticles. The PhC structure strengthens the optical field near the RERS hotspots and results in enhanced SERS signals from analytes. As an exemplary demonstration, the sensor was used to measure creatinine spiked in artificial urine samples within its clinically relevant concentration ranges. The results show the limit of detection of 0.9 mg/dL. By combining and exploiting the photonic and nanofluidic characters of the IO PhC structure, the strategy of using gold nanoparticle incorporated IO PhC capillary for SERS POCT proves to be facile, sensitive and cost-effective, which will have a wide application in many fields like chromatography analysis, body fluid analysis, drug screening and environment and food security monitoring.

Acknowledgment

This paper was supported by National Natural Science Foundation of China (Grants 21073033, 21373046 and 21327902), Jiangsu Science and Technology Department (Grant no.2014707), Suzhou Science and Technology Project (Grants ZXG2013036) and the Program for New Century Excellent Talents in University.

Appendix A. Supplementary material

Supplementary data associated with this article can be found in the online version at http://dx.doi.org/10.1016/j.bios.2015.05.036.

References

Alba, M., Pazos-Perez, N., Vaz, B., Formentin, P., Tebbe, M., Correa-Duarte, M.A., Granero, P., Ferre-Borrull, J., Alvarez, R., Pallares, J., Fery, A., de Lera, A.R., Marsal, L.F., Alvarez-Puebla, R.A., 2013. Macroscale plasmonic substrates for highly sensitive surface-enhanced Raman scattering. Angew. Chem. Int. Ed. 52 (25), 6459–6463.

Chanda, D., Shigeta, K., Truong, T., Lui, E., Mihi, A., Schulmerich, M., Braun, P.V., Bhargava, R., Rogers, J.A., 2011. Coupling of plasmonic and optical cavity modes in quasi-three-dimensional plasmonic crystals. Nat. Commun. 2, 479.

De Angelis, F., Gentile, F., Mecarini, F., Das, G., Moretti, M., Candeloro, P., Coluccio, M. L., Cojoc, G., Accardo, A., Liberale, C., Zaccaria, R.P., Perozziello, G., Tirinato, L., Toma, A., Cuda, G., Cingolani, R., Di Fabrizio, E., 2011. Breaking the diffusion limit with super-hydrophobic delivery of molecules to plasmonic nanofocusing SERS structures. Nat. Photonics 5 (11), 683–688.

Eric Le Ru, P.E., 2008. Principles of Surface-Enhanced Raman Spectroscopy: And related Plasmonic Effects. Elsevier Science.

Fan, X.D., White, I.M., 2011. Optofluidic microsystems for chemical and biological analysis. Nat. Photonics 5 (10), 591–597.

Ganesh, N., Zhang, W., Mathias, P.C., Chow, E., Soares, J.A.N.T., Malyarchuk, V., Smith, A.D., Cunningham, B.T., 2007. Enhanced fluorescence emission from quantum dots on a photonic crystal surface. Nat. Nanotechnol. 2 (8), 515–520.

Gervais, L., de Rooij, N., Delamarche, E., 2011. Microfluidic chips for point-of-care immunodiagnostics. Adv. Mater. 23 (24), H151–H176.

Gubala, V., Harris, L.F., Ricco, A.J., Tan, M.X., Williams, D.E., 2012. Point of Care Diagnostics: Status and Future. Anal Chem 84 (2), 487–515.

Guo, Y.B., Oo, M.K.K., Reddy, K., Fan, X.D., 2012. Ultrasensitive optofluidic surface-enhanced raman scattering detection with flow-through multihole capillaries. ACS Nano 6 (1), 381–388.

Hou, J., Zhang, H.C., Yang, Q., Li, M.Z., Song, Y.L., Jiang, L., 2014. Bio-inspired photonic-crystal microchip for fluorescent ultratrace detection. Angew. Chem. Int. Ed. 53 (23), 5791–5795.

Krug, J.T., Wang Sr, G.D., Nie, S.M., E., 1999. Efficient Raman enhancement and intermittent light emission observed in single gold nanocrystals. J. Am. Chem. Soc. 121 (39), 9208–9214.

Oh, Y.J., Jeong, K.H., 2014. Optofluidic SERS chip with plasmonic nanoprobes self-aligned along microfluidic channels. Lab Chip 14 (5), 865–868.

Oo, M.K.K., Guo, Y.B., Reddy, K., Liu, J., Fan, X.D., 2012. Ultrasensitive vapor detection with surface-enhanced Raman scattering-active gold nanoparticle immobilized flow-through multihole capillaries. Anal. Chem. 84 (7), 3376–3381.

Schlucker, S., 2014. Surface-enhanced Raman spectroscopy: concepts and chemical applications. Angew. Chem. Int. Ed. 53 (19), 4756–4795.

Schmidt, H., Hawkins, A.R., 2011. The photonic integration of non-solid media using optofluidics. Nat. Photonics 5 (10), 598–604.

Schroden, R.C., Al-Daous, M., Blanford, C.F., Stein, A., 2002. Optical properties of inverse opal photonic crystals. Chem. Mater. 14 (8), 3305–3315.
Schumacher, S., Nestler, J., Otto, T., Wegener, M., Ehrentreich-Forster, E., Michel, D., Wunderlich, K., Palzer, S., Sohn, K., Weber, A., Burgard, M., Grzesiak, A., Teichert, A., Brandenburg, A., Koger, B., Albers, J., Nebling, E., Bier, F.F., 2012. Highly-integrated lab-on-chip system for point-of-care multiparameter analysis. Lab Chip 12 (3), 464–473.
Shen, W.Z., Li, M.Z., Wang, B.L., Liu, J., Li, Z.Y., Jiang, L., Song, Y.L., 2012. Hierarchical optical antenna: Gold nanoparticle-modified photonic crystal for highly-sensitive label-free DNA detection. J. Mater. Chem. 22 (16), 8127–8133.
Sun, J.S., Xianyu, Y.L., Jiang, X.Y., 2014. Point-of-care biochemical assays using gold nanoparticle-implemented microfluidics. Chem. Soc. Rev. 43 (17), 6239–6253.
Surdo, S., Merlo, S., Carpignano, F., Strambini, L.M., Trono, C., Giannetti, A., Baldini, F., Barillaro, G., 2012. Optofluidic microsystems with integrated vertical one-dimensional photonic crystals for chemical analysis. Lab Chip 12 (21), 4403–4415.
Wade, J.H., Bailey, R.C., 2014. Refractive index-based detection of gradient elution liquid chromatography using chip-integrated microring resonator arrays. Anal. Chem. 86 (1), 913–919.
Wang, H., Malvadkar, N., Koytek, S., Bylander, J., Reeves, W.B., Demirel, M.C., 2010. Quantitative analysis of creatinine in urine by metalized nanostructured parylene. J. Biomed. Opt. 15 (2), 027004.
Wang, Y., Rauf, S., Grewal, Y.S., Spadafora, L.J., Shiddiky, M.J.A., Cangelosi, G.A., Schlucker, S., Trau, M., 2014. Duplex microfluidic SERS detection of pathogen antigens with nanoyeast single-chain variable fragments. Anal. Chem. 86 (19), 9930–9938.
Wustholz, K.L., Henry, A.I., McMahon, J.M., Freeman, R.G., Valley, N., Piotti, M.E., Natan, M.J., Schatz, G.C., Van Duyne, R.P., 2010. Structure–activity relationships in gold nanoparticle dimers and trimers for surface-enhanced Raman spectroscopy. J. Am. Chem. Soc. 132 (31), 10903–10910.
Yazdi, S.H., White, I.M., 2012. Optofluidic surface enhanced Raman spectroscopy microsystem for sensitive and repeatable on-site detection of chemical contaminants. Anal. Chem. 84 (18), 7992–7998.
Zhu, H.Y., Isikman, S.O., Mudanyali, O., Greenbaum, A., Ozcan, A., 2013. Optical imaging techniques for point-of-care diagnostics. Lab Chip 13 (1), 51–67.